optica

Architecture for the photonic integration of an optical atomic clock

Zachary L. Newman,[1,*] Vincent Maurice,[1] Tara Drake,[1] Jordan R. Stone,[1,2] Travis C. Briles,[1] Daryl T. Spencer,[1] Connor Fredrick,[1,2] Qing Li,[3] Daron Westly,[3] B. R. Ilic,[3] Boqiang Shen,[4] Myoung-Gyun Suh,[4] Ki Youl Yang,[4] Cort Johnson,[5] David M. S. Johnson,[5] Leo Hollberg,[6] Kerry J. Vahala,[4] Kartik Srinivasan,[3] Scott A. Diddams,[1,2] John Kitching,[1] Scott B. Papp,[1,2] and Matthew T. Hummon[1]

[1]National Institute of Standards and Technology, Boulder, Colorado 80305, USA
[2]Department of Physics, University of Colorado Boulder, Boulder, Colorado 80309, USA
[3]Center for Nanoscale Science and Technology, National Institute of Standards and Technology, Gaithersburg, Maryland 20899, USA
[4]California Institute of Technology, Pasadena, California 91125, USA
[5]Charles Stark Draper Laboratories, Cambridge, Massachusetts 02139, USA
[6]Stanford University, Stanford, California 94305, USA
*Corresponding author: zachary.newman@nist.gov

Laboratory optical atomic clocks achieve remarkable accuracy (now counted to 18 digits or more), opening possibilities for exploring fundamental physics and enabling new measurements. However, their size and the use of bulk components prevent them from being more widely adopted in applications that require precision timing. By leveraging silicon-chip photonics for integration and to reduce component size and complexity, we demonstrate a compact optical-clock architecture. Here a semiconductor laser is stabilized to an optical transition in a microfabricated rubidium vapor cell, and a pair of interlocked Kerr-microresonator frequency combs provide fully coherent optical division of the clock laser to generate an electronic 22 GHz clock signal with a fractional frequency instability of one part in 10^{13}. These results demonstrate key concepts of how to use silicon-chip devices in future portable and ultraprecise optical clocks.   © 2019 Optical Society of America under the terms of the OSA Open Access Publishing Agreement

https://doi.org/10.1364/OPTICA.6.000680

1. INTRODUCTION

Optical atomic clocks, which rely on high-frequency, narrow-linewidth optical transitions to stabilize a clock laser, outperform their microwave counterparts by several orders of magnitude due to their inherently large quality factors [1]. Optical clocks based on laser-cooled and lattice-trapped atoms have demonstrated fractional instabilities at the 10^{-18} level [2], setting stringent new limits on tests of fundamental physics [3,4], and may eventually replace microwave clocks in global timekeeping, navigation, and the definition of the SI second [5]. Despite their excellent performance, optical clocks are almost exclusively operated by metrological institutions and universities due to their large size and complexity.

Although significant progress has been made in reducing the size of laser-cooled atomic clocks to fit inside a mobile trailer [6], applications of these clocks are still limited to metrological clock comparisons and precision geodesy [7]. In contrast, optical oscillators referenced to thermal atomic or molecular vapors can be realized in small form factors and still reach instabilities below 10^{-14} [8,9]. A fully integrated optical clock would benefit many of the applications [10] that currently utilize compact or chip-scale [11]

microwave atomic clocks but, until recently, techniques for on-chip laser stabilization to atoms [12] and optical frequency division [13] were not available. Here, we propose and demonstrate an architecture for an integrated optical clock based on an atomic vapor cell implemented on a silicon chip and a microresonator frequency comb ("microcomb") system for optical frequency division. Experimentally, this consists of a semiconductor laser local oscillator locked to the rubidium-87 two-photon transition at 385.284 THz that is coherently divided down to a 22 GHz clock tone by stabilizing a pair of interlocked microcombs to the local oscillator.

Microcombs, optical-frequency combs that utilize four-wave mixing of a continuous-wave pump laser inside a high-Q optical microresonator, can be made to operate over a wide range of repetition rates, from ≈10 GHz to 1 THz [14]. In addition to their small size, microresonator combs are compatible with wafer-level manufacturing techniques and can operate at relatively low pump powers (tens of milliwatts) [15,16] compared with fiber and free-space frequency combs, making them an ideal choice for compact optical clocks and low-noise oscillators [13,17,18]. As part of prior work in our group, Papp et al. [13] demonstrated the first optical clock based on a microcomb by stabilizing two modes of a 33 GHz silica (SiO_2) microresonator to the D2 and D1 optical

transitions in Rb at 780 and 795 nm, respectively. However, due to the lack of self-referencing [19], the full stability of the optical standard was not transferred to the microwave domain. Recent progress in the field of microcombs has led to the realization of mode-locked, low-noise comb generation via temporal soliton formation in the resonator [20–22]. These dissipative Kerr-soliton (DKS) frequency combs have been used to demonstrate octave-spanning comb operation [23,24], self-referencing [25–27], and carrier-offset-frequency (f_{ceo}) phase stabilization [28–30]. To date, octave-spanning operation has only been demonstrated using combs with ≈1 THz repetition rates, well outside the bandwidth of traditional electronic detectors, a requirement for producing a usable microwave clock signal. To circumvent this issue, our optical clock architecture employs two interlocked microcombs: a high repetition rate, octave-spanning comb used for self-referencing, and a narrowband comb used to produce an electronically detectable microwave output.

2. EXPERIMENTAL METHODS

Figure 1(a) shows a simplified schematic of the experiment. The local oscillator ("clock laser") for our clock is a 778.1 nm, distributed Bragg reflector (DBR) laser that is referenced to the two-photon transition in ^{87}Rb in a microfabricated vapor cell. We generate a 1 THz repetition rate, octave-spanning, DKS frequency comb by coupling ≈100 mW of pump light from a 1.54 μm external cavity diode laser (ECDL) into a Si_3N_4 (SiN) microresonator, which is used for coarse optical division. Full stabilization of the SiN comb is accomplished by stabilizing f_{ceo} and locking an optical mode of the comb to the clock laser. We independently generate a narrowband, 22 GHz repetition rate, DKS comb by coupling ≈160 mW of light from a 1.556 μm ECDL

via tapered optical fiber into a silica microresonator. The two combs are then interlocked, and we use the silica comb as a finely spaced ruler to measure the repetition rate of the SiN comb. The output of the clock is a 22 GHz optical pulse train (and corresponding electrical signal) that is phase-stabilized to the Rb two-photon transition. The techniques for locking the DBR laser to the Rb atoms and stabilizing the frequency combs are detailed in Supplement 1. Figures 1(b)–1(d) show images of the main components of the clock: the two microresonators and the Rb cell. All three elements are microfabricated devices, and, in future implementations of the concept introduced here, would support more advanced integration.

The two-photon transition in Rb (Fig. 2 inset) has been studied extensively for use as an optical frequency standard [31–34]. Here, we only discuss details of this system relevant to spectroscopy in a microfabricated vapor cell. The clock laser is locked to the $5S_{1/2}$ (F = 2) to $5D_{5/2}$ (F = 4) two-photon transition in ^{87}Rb at 778.106 nm (385.284566 THz) using a 3 × 3 × 3 mm vapor cell [Fig. 1(d)]. The rear window of the cell is covered with a high-reflectivity coating (R = 99.8%), which is used to retro-reflect the clock laser and provide the counterpropagating beams required to excite the Doppler-free, two-photon transition. The front window is antireflection-coated on both sides to prevent parasitic reflections.

Excitation of the two-photon transition is detected via fluorescence at 420 nm from the 5D to 6P to 5S decay path by a microfabricated photomultiplier tube (PMT) along the optical axis of the clock laser. Figure 2 shows the output of the PMT as the clock laser is swept across the clock transition. A Lorentzian fit (purple) to the fluorescence signal gives a linewidth of ≈1 MHz, which includes contributions of 330 kHz from the natural linewidth, ≈475 kHz from the laser linewidth, ≈100 kHz of transit time
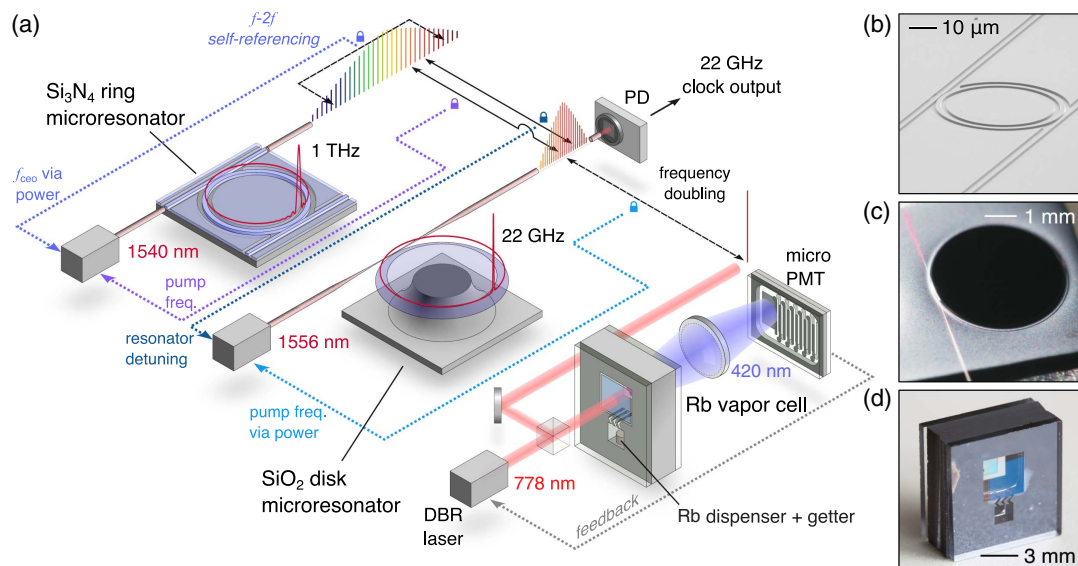
Fig. 1. Schematic of the microfabricated photonic optical atomic clock. (a) The microfabricated optical clock consists of an optical local oscillator, a microfabricated Rb vapor cell, and a pair of microresonator frequency combs, which serve as optical clockwork. Absorption of the clock laser in the cell is detected via the collection of 420 nm fluorescence using a microfabricated PMT. The optical clockwork consists of interlocked DKS combs generated using a ≈2 mm diameter, silica microresonator, and a 46 μm diameter, SiN microresonator. Stabilization of the frequency combs' output is performed via electronic feedback (indicated by dotted lines) to the pump frequency and resonator detuning of the ECDLs used to pump the microresonators. The feedback signals are generated from optical heterodyne beat notes of adjacent comb teeth, as indicated by the solid black arrows. In some cases, frequency doubling (dashed black arrows) was required to compare optical signals. For simplicity, we do not picture the frequency and intensity modulators used for feedback in the comb frequency servo loops. (b) Scanning-electron microscope image of the SiN microresonator. Photographs of (c) the silica microresonator and (d) the microfabricated Rb vapor cell.
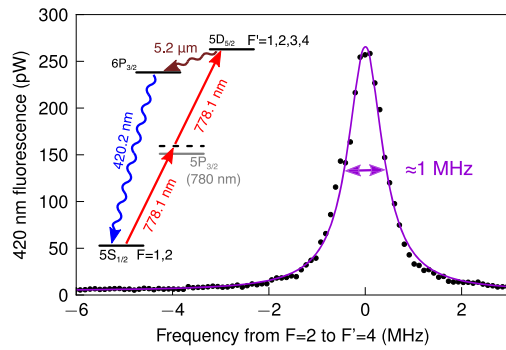
Fig. 2. Spectroscopy of optical clock transition. Doppler-free fluorescence spectroscopy of the optical clock transition between the $5S_{1/2}$, F = 2 to $5D_{5/2}$, F = 4 levels at 385.284566 THz, with a full width at half-maximum of $\approx$1 MHz. The atomic level structure of the ^{87}Rb two-photon transition is shown as an inset.

broadening [35], and $\approx$100 kHz due to collisional broadening from background gases in the cell (see Supplement 1).

Figures 3(a) and 3(b) show optical spectra of the free-running soliton combs. During clock operation, the silica comb pump laser, $\nu_{GHz,pump}$, is frequency-doubled and subsequently phase-locked to the clock laser, ν_{Rb}. The SiN comb tooth at 1556 nm ($\nu_{THz,pump-2}$) is then locked to $\nu_{GHz,pump}$. Here, $\nu_{GHz/THz,pump-n}$, describes the silica/SiN (GHz/THz) comb tooth n modes on the low-frequency side of the pump. We lock the terahertz comb offset frequency, f_{ceo}, with an ECDL-assisted, f-$2f$ interferometer [29]. Simultaneous stabilization of the SiN comb offset frequency and repetition rate (via $\nu_{THz,pump-2}$ locked to ν_{Rb}) effectively divides the clock laser from 385 to 1 THz. We complete the optical frequency division by phase locking $\nu_{GHz,pump-48}$ to $\nu_{THz,pump-3}$ at 1564 nm, which

generates a stable, Rb-referenced, 22 GHz clock output tone. Figure 3(c) shows the beat note between the 22 GHz clock output and a 22 GHz signal referenced to a hydrogen maser.

The frequency of the clock output, $f_{GHz,rep}$, is directly linked to the Rb two-photon transition and is given by the simple relationship,

$$f_{GHz,rep} = \frac{\nu_{Rb} + (\alpha/2 + 2 \cdot [(q-1) \cdot \beta + q \cdot \gamma - \delta]) \cdot f_{10\,MHz}}{2 \cdot q \cdot p},$$

(1)

where ν_{Rb} is the clock laser frequency, $q = 190$ is the mode number of the SiN comb line closest to the clock transition $\nu_{THz,pump-2}$, and $p = 48$ is the number of 22 GHz comb modes separating the lock points to the SiN comb teeth, $\nu_{THz,pump-2}$, and $\nu_{THz,pump-3}$. The synthesizer frequencies used in each of the phase locks between the comb teeth are defined in terms of the ratios of integers α, β, γ, and δ relative to a 10 MHz clock referenced to a hydrogen maser, $f_{10\,MHz}$, as indicated in Fig. 3(b). The denominator in Eq. (1) gives the full division factor of the comb: $n = 2 \times 48 \times 190 = 18,240$. A crystal oscillator referenced to the free-running repetition rate of the silica comb [Fig. 4(b), open green squares] can instead be used as a reference for phase locking the microcombs, and the clock can be run with no external frequency references.

3. RESULTS AND DISCUSSION

Figure 4 summarizes the performance of the optical clock. Figure 4(a) shows a plot of the 22 GHz clock output measured against the hydrogen maser and multiplied up to the optical domain (blue), along with a plot of the clock laser frequency measured against an auxiliary erbium fiber frequency comb (orange)
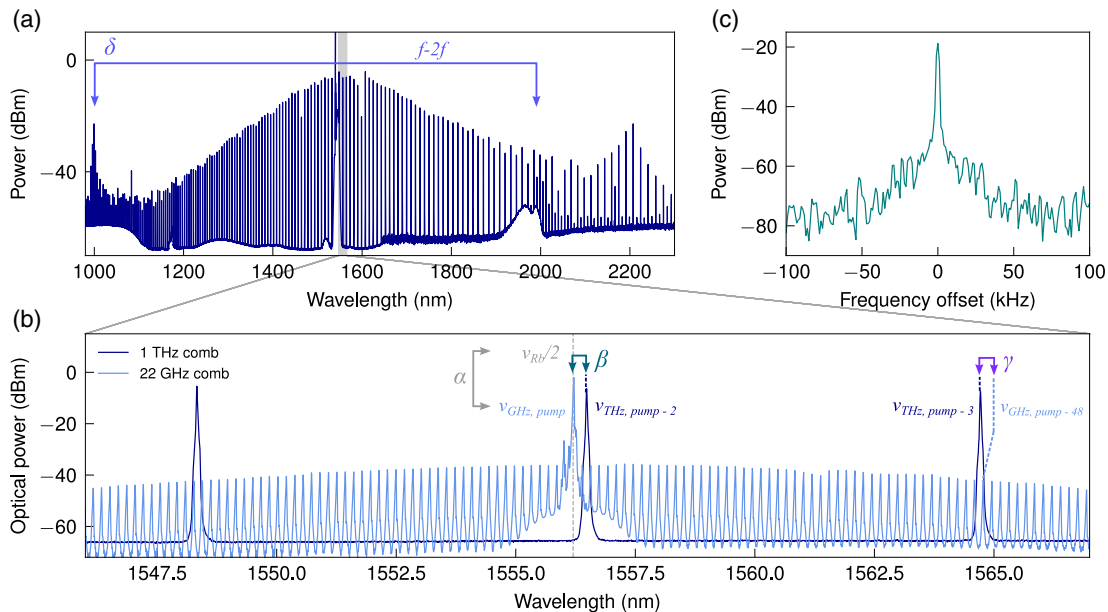
Fig. 3. Microcomb spectra. (a) SiN microresonator comb spectrum, showing the 1 THz comb tooth spacing with a resolution bandwidth of $\Delta\lambda = 0.1$ nm. An f-$2f$ interferometer (light blue arrow) in which light at 1998 nm is frequency-doubled to heterodyne with the comb teeth in the dispersive wave at 999 nm is used to measure and stabilize the offset frequency, f_{ceo}, of the SiN comb ($\delta = f_{ceo}/10$ MHz). (b) Silica microresonator comb spectrum (light blue) with 22 GHz repetition rate, shown overlaid with three teeth from the 1 THz, SiN comb (dark blue), with a resolution of $\Delta\lambda = 0.02$ nm. Arrows indicate phase locks used to stabilize the combs. Greek letters show the ratio-of-integer values multiplied by a 10 MHz clock that are used as a reference for each of the phase locks. For the devices used in the experiment, $\alpha = 154.224$, $\beta = 3525.29238$, $\gamma = 539.9808$, and $\delta = -1280.0$. (c) RF spectrum of the 22 GHz clock output.
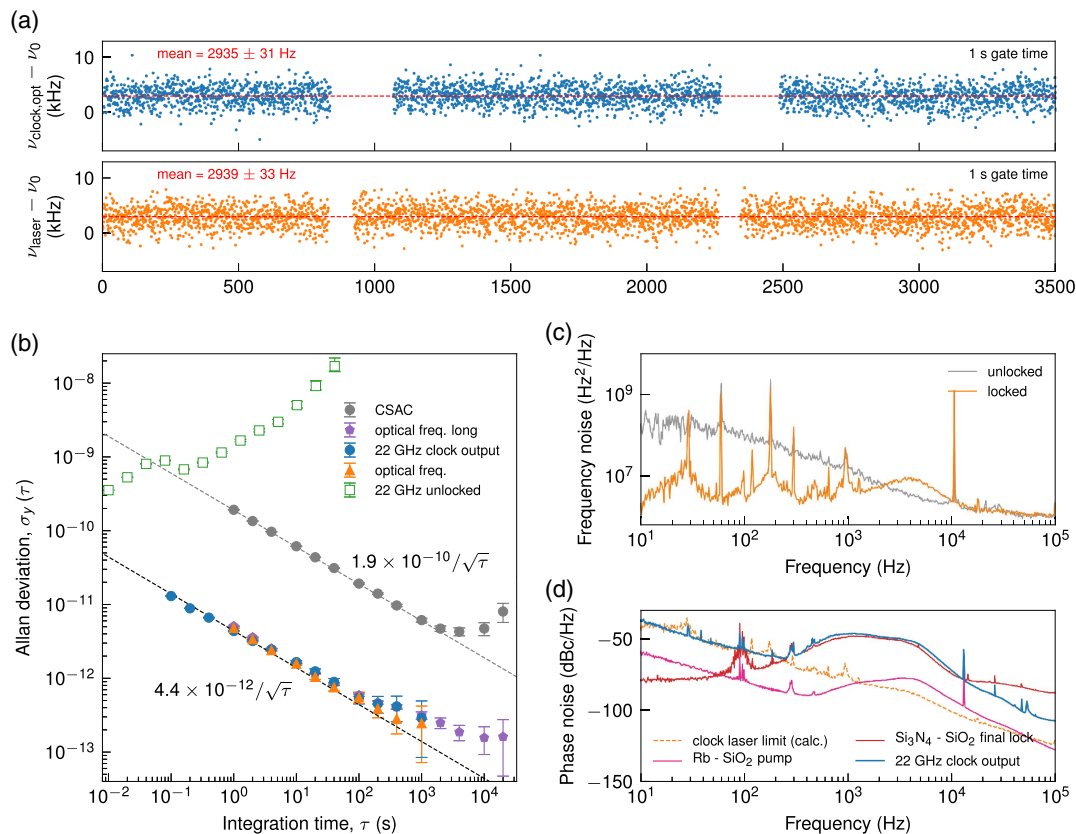
Fig. 4. Optical clock performance. (a) Time-series measurement of the clock optical frequency offset derived from the 22 GHz clock output frequency, $\nu_{\mathrm{clock,opt}}$ (top, blue) and derived from the beat note against the Er:fiber frequency comb, ν_{laser} (bottom, orange). The reference frequency is $\nu_o = 385284566370400$ Hz [34]. Short breaks in the data indicate periods where the clock laser dropped out of lock. (b) Comparison of Allan deviation of 22 GHz clock output for the free-running silica microresonator (green open squares), the fully stabilized comb (blue circles), and the heterodyne beat note of the clock laser with the Er:fiber comb (orange triangles). At long integration times (purple pentagons), the clock stability is limited to $\approx 1 \times 10^{-13}$ due to temperature fluctuations in the lab. Error bars represent a 68% confidence interval. An Allan deviation of a Microsemi chip-scale atomic clock (CSAC) measured against a hydrogen maser is shown for comparison (gray circles). (c) Frequency noise spectra for the free-running and locked clock laser. A large servo bump at ≈ 4 kHz is evidence of frequency noise spectra. (d) Phase noise away from carrier for the 22 GHz clock output signal (blue), along with the contributions from the intermediate phase locks (red and magenta) and the phase noise of the clock laser calculated from the laser frequency noise spectrum (orange dashed), which gives a lower limit on the phase noise of the 22 GHz clock output.

as an independent confirmation of the clock accuracy. The mean values of the two measurements of the clock frequency agree to within their standard error. The absolute frequency shift of our clock relative to the BIPM accepted value [34], after accounting for the light shift and the Rb–Rb collision shift is $\Delta\nu \approx 2.9 \pm 7.9$ kHz $(\Delta\nu/\Delta\nu_{\mathrm{Rb}} \approx 8 \times 10^{-12})$, and is primarily due to the collision shift from background gases in the cell (an uncertainty budget is included in Supplement 1). It is worth noting that this represents the first measurement of an absolute clock transition frequency in a chip-scale vapor cell.

Figure 4(b) shows an Allan deviation of the fully stabilized clock signal [Fig. 4(a), blue] measured against the hydrogen maser along with an Allan deviation of the heterodyne of the clock laser with the fiber frequency comb [Fig. 4(a), orange]. An Allan deviation of the clock laser frequency measured against the fiber comb for ≈ 24 h measured at a later date [purple] reflects the stability of the clock laser at longer integration times. The measured fractional frequency instability of the microwave output is $4.4 \times 10^{-12}/\tau^{1/2}$ and is limited by frequency noise on the DBR laser [Fig. 4(b)] via the intermodulation effect [36]. At long integration times ($>10^3$ s), we notice that fluctuations in the clock laser frequency are correlated

with the laboratory temperature and limit the ultimate stability of the clock to $\approx 1 \times 10^{-13}$.

Figure 4(d) shows the clock phase noise (along with that of the intermediate phase locks), which is competitive with high-frequency (tens of gigahertz) analog signal generators. At low frequencies (<300 Hz), the phase noise is limited by the intrinsic phase noise of the clock laser (consistent with perfect optical division at integration time >1 s), while the bump around 1 kHz results from the final phase lock between the silica and SiN combs. The phase noise at high frequencies (>10 kHz, outside the bandwidth of the comb-to-comb phase locks) is likely due to the silica comb pump laser [37]. This suggests the clock could be operated as a low-phase noise oscillator by utilizing narrow-linewidth pump sources.

4. CONCLUSION

In summary, we present a clear path towards the future integration of optical atomic clocks by proposing a framework for optical frequency division using microresonator frequency combs and have demonstrated a distributed optical atomic clock with a stability of $4.4 \times 10^{-12}/\tau^{1/2}$, where the critical components of the

clock are integrated devices. At present, the stability of our clock is limited by the performance of available, integrated 778 nm sources, but short-term stabilities near 10^{-13} at 1 s may be possible with low-noise lasers. We anticipate that devices such as integrated narrow-linewidth lasers [38–40] with fast frequency tuning rates and waveguide-based second-harmonic generators [41] will eventually replace the off-the-shelf components in our clock, making a fully integrated optical atomic clock viable. State-of-the-art chip-scale optical clocks would impact applications, including gravitational and remote sensing, timing and navigation when GPS is unreliable, the synchronization of large aperture networks for long-baseline interferometry [42–44] and enable *in situ*, SI-traceable calibrations of laboratory instruments.

See Supplement 1 for supporting content.

REFERENCES

1. S. A. Diddams, T. Udem, J. C. Bergquist, E. A. Curtis, R. E. Drullinger, L. Hollberg, W. M. Itano, W. D. Lee, C. W. Oates, K. R. Vogel, and D. J. Wineland, "An optical clock based on a single trapped ^{199}Hg$^+$ ion," Science **293**, 825–828 (2001).
2. M. Schioppo, R. C. Brown, W. F. McGrew, N. Hinkley, R. J. Fasano, K. Beloy, T. H. Yoon, G. Milani, D. Nicolodi, J. A. Sherman, N. B. Phillips, C. W. Oates, and A. D. Ludlow, "Ultrastable optical clock with two cold-atom ensembles," Nat. Photonics **11**, 48–52 (2016).
3. T. Rosenband, D. B. Hume, P. O. Schmidt, C. W. Chou, A. Brusch, L. Lorini, W. H. Oskay, R. E. Drullinger, T. M. Fortier, J. E. Stalnaker, S. A. Diddams, W. C. Swann, N. R. Newbury, W. M. Itano, D. J. Wineland, and J. C. Bergquist, "Frequency ratio of Al$^+$ and Hg$^+$ single-ion optical clocks; metrology at the 17th decimal place," Science **319**, 1808–1812 (2008).
4. R. M. Godun, P. B. R. Nisbet-Jones, J. M. Jones, S. A. King, L. A. M. Johnson, H. S. Margolis, K. Szymaniec, S. N. Lea, K. Bongs, and P. Gill, "Frequency ratio of two optical clock transitions in ^{171}Yb$^+$ and constraints on the time variation of fundamental constants," Phys. Rev. Lett. **113**, 210801 (2014).
5. F. Riehle, "Towards a redefinition of the second based on optical atomic clocks," Comptes Rendus Phys. **16**, 506–515 (2015).
6. S. B. Koller, J. Grotti, S. Vogt, A. Al-Masoudi, S. Dörscher, S. Häfner, U. Sterr, and C. Lisdat, "Transportable optical lattice clock with 7×10^{-17} uncertainty," Phys. Rev. Lett. **118**, 073601 (2017).
7. J. Grotti, S. Koller, S. Vogt, S. Häfner, U. Sterr, C. Lisdat, H. Denker, C. Voigt, L. Timmen, A. Rolland, F. N. Baynes, H. S. Margolis, M. Zampaolo, P. Thoumany, M. Pizzocaro, B. Rauf, F. Bregolin, A. Tampellini, P. Barbieri, M. Zucco, G. A. Costanzo, C. Clivati, F. Levi, and D. Calonico, "Geodesy and metrology with a transportable optical clock," Nat. Phys. **14**, 437–441 (2018).
8. T. Schuldt, K. Döringshoff, E. V. Kovalchuk, A. Keetman, J. Pahl, A. Peters, and C. Braxmaier, "Development of a compact optical absolute
9. frequency reference for space with 10^{-15} instability," Appl. Opt. **56**, 1101–1106 (2017).
9. K. W. Martin, G. Phelps, N. D. Lemke, M. S. Bigelow, B. Stuhl, M. Wojcik, M. Holt, I. Coddington, M. W. Bishop, and J. H. Burke, "Compact optical atomic clock based on a two-photon transition in rubidium," Phys. Rev. Appl. **9**, 014019 (2018).
10. J. R. Vig, "Military applications of high accuracy frequency standards and clocks," IEEE Trans. Ultrason. Ferroelectr. Freq. Control. **40**, 522–527 (1993).
11. S. Knappe, V. Shah, P. D. D. Schwindt, L. Hollberg, J. Kitching, L. A. Liew, and J. Moreland, "A microfabricated atomic clock," Appl. Phys. Lett. **85**, 1460–1462 (2004).
12. M. T. Hummon, S. Kang, D. G. Bopp, Q. Li, D. A. Westly, S. Kim, C. Fredrick, S. A. Diddams, K. Srinivasan, V. Aksyuk, and J. E. Kitching, "Photonic chip for laser stabilization to an atomic vapor with 10^{-11} instability," Optica **5**, 443–449 (2018).
13. S. B. Papp, K. Beha, P. Del'Haye, F. Quinlan, H. Lee, K. J. Vahala, and S. A. Diddams, "Microresonator frequency comb optical clock," Optica **1**, 10–14 (2014).
14. T. J. Kippenberg, A. L. Gaeta, M. Lipson, and M. L. Gorodetsky, "Dissipative Kerr solitons in optical microresonators," Science **361**, eaan8083 (2018).
15. J. Liu, A. S. Raja, M. Karpov, B. Ghadiani, M. H. P. Pfeiffer, N. J. Engelsen, H. Guo, M. Zervas, and T. J. Kippenberg, "Ultralow-power chip-based soliton microcombs for photonic integration," Optica **5**, 3–9 (2018).
16. B. Stern, X. Ji, Y. Okawachi, A. L. Gaeta, and M. Lipson, "Battery-operated integrated frequency comb generator," Nature **562**, 401–405 (2018).
17. A. A. Savchenkov, D. Eliyahu, W. Liang, V. S. Ilchenko, J. Byrd, A. B. Matsko, D. Seidel, and L. Maleki, "Stabilization of a Kerr frequency comb oscillator," Opt. Lett. **38**, 2636–2639 (2013).
18. W. Liang, D. Eliyahu, V. S. Ilchenko, A. A. Savchenkov, D. Seidel, L. Maleki, and A. B. Matsko, "High spectral purity Kerr frequency comb radio frequency photonic oscillator," Nat. Commun. **6**, 1–8 (2015).
19. D. J. Jones, S. A. Diddams, J. K. Ranka, A. Stentz, R. S. Windeler, J. L. Hall, and S. T. Cundiff, "Carrier-envelope phase control of femtosecond mode-locked lasers and direct optical frequency synthesis," Science **288**, 635–639 (2000).
20. T. Herr, V. Brasch, J. D. Jost, C. Y. Wang, N. M. Kondratiev, M. L. Gorodetsky, and T. J. Kippenberg, "Temporal solitons in optical microresonators," Nat. Photonics **8**, 145–152 (2013).
21. X. Yi, Q.-F. Yang, X. Zhang, K. Y. Yang, X. Li, and K. Vahala, "Single-mode dispersive waves and soliton microcomb dynamics," Nat. Commun. **8**, 14869 (2017).
22. S. Coen, H. G. Randle, T. Sylvestre, and M. Erkintalo, "Modeling of octave-spanning Kerr frequency combs using a generalized mean-field Lugiato-Lefever model," Opt. Lett. **38**, 37–39 (2013).
23. Q. Li, T. C. Briles, D. A. Westly, T. E. Drake, J. R. Stone, B. R. Ilic, S. A. Diddams, S. B. Papp, and K. Srinivasan, "Stably accessing octave-spanning microresonator frequency combs in the soliton regime," Optica **4**, 193–203 (2016).
24. M. H. P. Pfeiffer, C. Herkommer, J. Liu, H. Guo, M. Karpov, E. Lucas, M. Zervas, and T. J. Kippenberg, "Octave-spanning dissipative Kerr soliton frequency combs in Si$_3$N$_4$ microresonators," Optica **4**, 684–690 (2017).
25. J. D. Jost, T. Herr, C. Lecaplain, V. Brasch, M. H. P. Pfeiffer, and T. J. Kippenberg, "Counting the cycles of light using a self-referenced optical microresonator," Optica **2**, 706–711 (2015).
26. P. Del'Haye, A. Coillet, T. Fortier, K. Beha, D. C. Cole, K. Y. Yang, H. Lee, K. J. Vahala, S. B. Papp, and S. A. Diddams, "Phase-coherent microwave-to-optical link with a self-referenced microcomb," Nat. Photonics **10**, 516–520 (2016).
27. V. Brasch, E. Lucas, J. D. Jost, M. Geiselmann, and T. J. Kippenberg, "Self-referenced photonic chip soliton Kerr frequency comb," Light: Sci. Appl. **6**, e16202 (2017).
28. T. E. Drake, T. C. Briles, D. T. Spencer, J. R. Stone, D. R. Carlson, D. D. Hickstein, Q. Li, D. Westly, K. Srinivasan, S. A. Diddams, and S. B. Papp, "A Kerr-microresonator optical clockwork," arXiv:1811.00581 (2018).
29. T. C. Briles, J. R. Stone, T. E. Drake, D. T. Spencer, C. Frederick, Q. Li, D. A. Westly, B. R. Ilic, K. Srinivasan, S. A. Diddams, and S. B. Papp, "Interlocking Kerr-microresonator frequency combs for microwave to optical synthesis," Opt. Lett. **43**, 2933–2936 (2018).
30. D. T. Spencer, T. Drake, T. C. Briles, J. Stone, L. C. Sinclair, C. Frederick, Q. Li, D. Westly, B. R. Ilic, A. Bluestone, N. Volet, T. Komljenovic,

L. Chang, S. H. Lee, D. Y. Oh, M.-G. Suh, K. Y. Yang, M. H. P. Pfeiffer, T. J. Kippenberg, E. Norberg, L. Theogarajan, K. Vahala, N. R. Newbury, K. Srinivasan, J. E. Bowers, S. A. Diddams, and S. B. Papp, "An optical-frequency synthesizer using integrated photonics," Nature **557**, 81–85 (2018).

31. G. Grynberg and B. Cagnac, "Doppler-free multiphotonic spectroscopy," Rep. Prog. Phys. **40**, 791–841 (1977).

32. L. Hilico, R. Felder, D. Touahri, O. Acef, A. Clairon, and F. Biraben, "Metrological features of the rubidium two-photon standards of the BNM-LPTF and Kastler Brossel Laboratories," Eur. Phys. J. Appl. Phys. **4**, 219–225 (1998).

33. N. D. Zameroski, G. D. Hager, C. J. Erickson, and J. H. Burke, "Pressure broadening and frequency shift of the 5S 1/2 to 5D 5/2 and 5S 1/2 to 7S 1/2 two photon transitions in ^{85}Rb by the noble gases and N$_2$," J. Phys. B **47**, 225205 (2014).

34. J. E. Bernard, A. A. Madej, K. J. Siemsen, L. Marmet, C. Latrasse, D. Touahri, M. Poulin, M. Allard, and M. Tetu, "Absolute frequency measurement of a laser at 1556 nm locked to the 5S1/2-5D5/2 two-photon transition in 87-Rb," Opt. Commun. **173**, 357–364 (2000).

35. F. Biraben, M. Bassini, and B. Cagnac, "Line-shapes in Doppler-free two-photon spectroscopy the effect of finite transit time," J. Phys. **40**, 445–455 (1979).

36. C. Audoin, V. Candelier, and N. Dimarcq, "A limit to the frequency stability of passive frequency standards due to an intermodulation effect," IEEE Trans. Instrum. Meas. **40**, 121–125 (1991).

37. J. R. Stone, T. C. Briles, T. E. Drake, D. T. Spencer, D. R. Carlson, S. A. Diddams, and S. B. Papp, "Thermal and nonlinear dissipative-soliton dynamics in Kerr-microresonator frequency combs," Phys. Rev. Lett. **121**, 63902 (2018).

38. S. Gundavarapu, G. M. Brodnik, M. Puckett, T. Huffman, D. Bose, R. Behunin, J. Wu, T. Qiu, C. Pinho, N. Chauhan, J. Nohava, P. T. Rakich, K. D. Nelson, M. Salit, and D. J. Blumenthal, "Sub-hertz fundamental linewidth photonic integrated Brillouin laser," Nat. Photonics **13**, 60–67 (2018).

39. H. Guan, A. Novack, T. Galfsky, M. Yangjin, S. Fathololoumi, A. Horth, T. Huynh, J. Roman, R. Shi, M. Caverley, Y. Liu, T. Baehr-Jones, K. Bergman, and M. Hochberg, "Widely-tunable, narrow-linewidth III-V/silicon hybrid external-cavity laser for coherent communication," Opt. Express **26**, 7920–7933 (2018).

40. P. A. Morton and M. J. Morton, "High-power, ultra-low noise hybrid lasers for microwave photonics and optical sensing," J. Lightwave Technol. **36**, 5048–5057 (2018).

41. X. Guo, C.-L. Zou, and H. X. Tang, "Second-harmonic generation in aluminum nitride microrings with 2500%/W conversion efficiency," Optica **3**, 1126–1131 (2016).

42. F. Riehle, "Optical clock networks," Nat. Photonics **11**, 25–31 (2017).

43. J. Ye, J.-L. Peng, R. J. Jones, K. W. Holman, J. L. Hall, D. J. Jones, S. A. Diddams, J. Kitching, S. Bize, J. C. Bergquist, L. W. Hollberg, L. Robertsson, and L.-S. Ma, "Delivery of high-stability optical and microwave frequency standards over an optical fiber network," J. Opt. Soc. Am. B **20**, 1459–1467 (2003).

44. C. Clivati, G. A. Costanzo, M. Frittelli, F. Levi, A. Mura, M. Zucco, R. Ambrosini, C. Bortolotti, F. Perini, M. Roma, and D. Calonico, "A coherent fiber link for very long baseline interferometry," IEEE Trans. Ultrason. Ferroelectr. Freq. Control **62**, 1907–1912 (2015).